

# Enhancing Task Classification in Human-Machine Collaborative Teleoperation Systems by Real-time Evaluation of an Agreement Criterion

Carolina Passenberg\*  
cpassenberg@lrs.ei.tum.de

Nikolay Stefanov\*  
nikolay.stefanov@tum.de

Angelika Peer\*  
angelika.peer@tum.de

Martin Buss\*  
m.buss@ieee.org\*

## ABSTRACT

Human-machine collaborative teleoperation systems were introduced to overcome limitations of state-of-the-art teleoperation systems by using a virtual assistant that supports the human operator in the execution of a task. Since assistances are highly task-dependent a correct classification of the currently performed task is paramount. In this paper, we present a novel approach for improving task classification for a human-machine collaborative teleoperation system. Starting from a classical HMM-based classifier implemented in our previous research, we introduce a method for correcting erroneous task classifications by evaluating an agreement criterion. This criterion is based on interactive forces and is used to distinguish between situations in which human and assistant agree/disagree in their execution of the task. Using disagreement as indicator for the activation of an unsuitable/suboptimal assistance, erroneous task classifications are identified and the original classification result is revised. The proposed approach shows significant improvements in task classification coming along with a comparable low implementation effort.

## 1 INTRODUCTION

In a haptic teleoperation system, a human operator performs complex manipulation tasks in a remote environment via a teleoperator while receiving haptic feedback from the interaction with the environment, see Fig. 1. Despite recent advances in the field, state-of-the-art teleoperation systems are still characterized by a long execution time, high failure rate, and low performance compared to direct human manipulation. In order to overcome these limitations, virtual assistants have been introduced to support the human operator in the execution of a task. Several types of assistances have been proposed in the past ranging from simple visual overlays, over stabilizing controllers to haptic guiding systems, see [1] for an overview. The variety of assistance functions developed and proposed in literature clearly shows that no universal assistance function exists, but rather different tasks require the activation of different assistances. While manual activation of assistances is a valuable strategy, recent investigations aim for an automatic task classification and assistance function activation. Hidden Markov Models (HMM) have been widely used in this context. Originally applied to problems in speech recognition, recently HMMs have been also implemented for human-machine collaborative teleoperation systems [2, 3, 4, 5, 6, 7]. Classification methods based on HMMs are known for their robustness against variations in task execution, their low computational effort as well as their adaptation and generalization capability to a broad area of tasks.

In our previous research we implemented an HMM-based task recognition algorithm to distinguish between a series of pre-defined tasks [7]. Depending on the task, correct recognition rates of about 89 % were obtained. While operation was smooth when correct

\*The authors are with the Institute of Automatic Control Engineering, Technische Universität München, Germany.

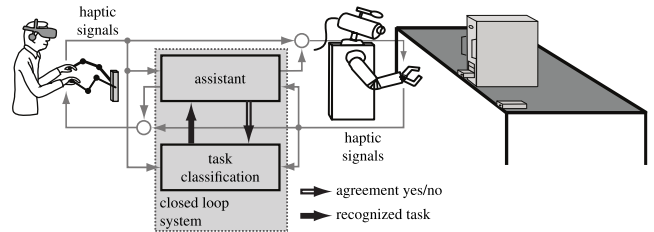


Figure 1: Feedback loop from the haptic assistant to the task classification

assistances were activated, a wrong task classification resulted in the activation of unsuitable or sub-optimal assistance functions, which caused a drop in task performance or even made the execution fail. Especially when applying haptic assistances, an assistance well suited for one type of task can cause instability when applied to another. Thus, errors in task recognition should be minimized not only to optimize task performance, but also to guarantee stable operation.

Inspired by approaches found in the field of brain-computer interfaces (BCI) that evaluate error-related potentials to correct the original classification result [8, 9], in this work, we introduce a method for correcting erroneous task classifications in a human-machine collaborative teleoperation system (see Fig. 1) by evaluating an agreement criterion. Similar to the error-related potential that indicates when an intention was wrongly classified, the agreement criterion will serve as a measure to indicate whether human operator and assistance functions generally agree or disagree in the execution of a task. A disagreement is interpreted as indicator for an unsuitable or suboptimal activated assistance and thus, a wrong task classification. In case the criterion indicates a disagreement the classification result will be revised with the aim of correcting the original decision. Following this procedure an overall improved classification can be achieved.

The paper is structured as follows: The proposed approach, the scenario, the design of the task-specific assistance functions, and the task classification algorithm are presented in Sec. 2. The experimental setup used to evaluate the effectiveness of the proposed approach as well as obtained results are detailed and discussed in Sec. 3. The paper closes with a summary and outlook to future research.

## 2 CONCEPT & METHODS

In correspondence to the error-related potential that is activated when intentions are wrongly classified, we look for a criterion that allows detecting the activation of unsuitable or sub-optimal assistance functions when performing a haptic interaction task. In [10], we found that interactive forces between human and assistant can be used to distinguish between cases where human/assistant agree or disagree in their execution of a task. In this work an adapted version of this criterion, denoted as *DC*, is used in order to identify a disagreement and thus, a wrong classification of the performed task. In case disagreement between human and assistant is detected, the

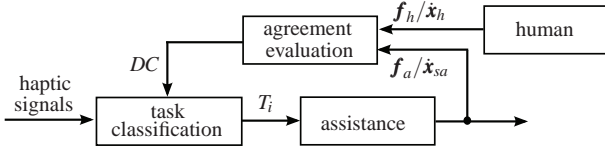


Figure 2: Task classification correction based on agreement criterion

original classification result will be revised and the next most likely task will be selected. As shown in Fig. 2 the agreement criterion  $DC$  acts as direct feedback to the task classifier.

In the following subsections, we introduce the teleoperation scenario that has been used to test our approach, list the single tasks it consists of, describe the assistance functions we have designed for them, shortly review our task classification algorithm implemented in our previous research as well as introduce our new correction procedure adopted to enhance the original task classification. Since the assistance algorithms as well as the task classifier used in our study are highly task-dependent, we start with the description of the overall scenario.

## 2.1 Scenario

The replacement of a defective hard drive is considered as exemplary scenario to evaluate our approach. The scenario requires the sequential execution of four different tasks: transportation (T2), positioning (T3), carrying (T4), and idle (T1), see Fig. 3.

At the beginning the operator pulls the broken hard drive out of the rack. This is associated with a transportation task. It is a typical example for movements in constrained environments and is characterized by large sliding friction effects. In a second step, the hard drive is carried from the rack to a predefined position where it is dropped. The operator takes the new hard drive and carries it back to the rack. This phase is called carrying and is performed in free space. In this phase, only the hard drive's mass is measured on the remote site. Next, the hard drive needs to be inserted back into the rack corresponding to another transportation task. Finally, the hard drive has to be positioned precisely at the target location, so that the holes of the drive and the rack coincide and it can be fixed using bolts. The main physical effects the operator has to deal with in this phase are slip and stick effects caused by the static friction between object and rack. The idle state (T1) is active whenever no contact with the hard drive occurs.

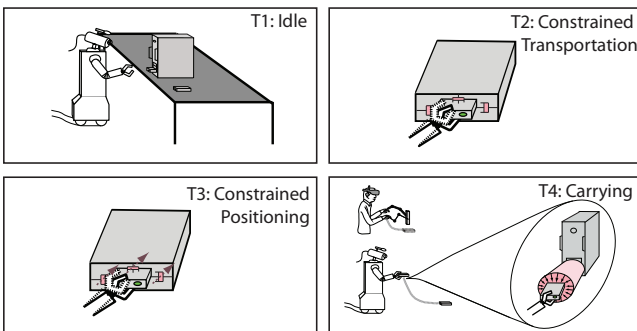


Figure 3: Scenario consisting of four tasks: Idle, Transportation, Positioning, Carrying

## 2.2 Assistance

In order to support the execution of the tasks, we implemented assistance functions for T2-T4. Since the scenario can be per-

formed using translational movements only, these degrees of freedom (DOF) are considered for the design of the assistance functions. Rotational movements are constrained by a strong virtual mass-spring-damper dynamics. The assistance functions act as additional virtual forces  $f_a$  or velocities  $\dot{x}_a$  to the human applied forces/velocities, see Fig. 8.

**T2 Transportation:** For transportation tasks, the most important objective is to ensure stability while performing motions in highly constrained environments. This is realized by introducing additional virtual damping of  $d^{T2} = 30$  Ns/m to each direction of motion. Furthermore, as the main constrained direction of motion is the up/down axis, forces applied by the human in this direction are reduced by 90%.

**T3 Positioning:** Positioning is performed in the same constrained environment than transportation, and thus, the same assistance as for the transportation task is used. The dominating physical effect in this task, however, are slip and stick effects. These effects complicate small-scale motions as required for positioning tasks resulting in large task completion times and large applied forces. Thus, in order to overcome the slip and stick effects, the resolution in the lower force range is increased by amplifying the human forces applied in the horizontal plane by a factor 2.

**T4 Carrying:** In this task, the main objective is to realize a high task performance, i.e. fast task execution with low effort. The carrying task exhibits two main components: large free space motions for carrying the hard drive and small-scale motions for positioning the hard drive in front of the rack. For positioning the hard drive, a potential field is useful to guide the operator towards the hole of the rack. Potential fields provide the operator with haptic cues to drive him/her towards or away from selected regions, see [11, 12]. In this paper, a potential field is used to guide the operator towards the hole of the rack, where the hard drive needs to be inserted. If the hard drive is grasped for the first time, its position is registered and later used to render a cylindrical attracting potential field around this position. We selected a cylinder with a diameter of 12 cm. A virtual spring-damper dynamics with spring constant  $k_{pf}^{T4} = 200$  N/m and damping constant  $d_{pf}^{T4} = 25$  Ns/m is fixed between the center line of the cylinder and the position of the teleoperator. Regarding the first component of the carrying task, facilitation of large motions in free space, the commanded teleoperator velocity is scaled up by a factor 1.5 in all directions and the virtual mass-damper dynamics of the nominal controller is reduced by  $m_a^{T4} = 2$  kg and  $d_a^{T4} = 50$  Ns/m.

## 2.3 Task classification

Our task classification algorithm is based on a Hidden Markov Model (HMM) approach. A thorough theoretical overview of HMMs and their applicability to classification problems in speech recognition can be found in [13]. Due to its simple implementation, robustness and high invariance against time warping, their applicability extends far beyond speech recognition and thus, HMMs have been applied to a variety of classification problems, including classification in haptic interaction, see e.g. [14].

An HMM is a simple belief network with hidden states exhibiting Markov property. It is represented by a probability distribution over a finite sequence of observations (output alphabet). An HMM is often denoted as a tuple  $\lambda = (Q, V, \pi, A, B)$ . It is fully defined by specifying the set of hidden states  $Q$ , the set of output symbols  $V$ , its initial state probability distribution vector  $\pi$ , the matrix of state transition distribution  $A$  and the emission probability distribution matrix  $B$ .

Knowing matrices  $A$  and  $B$  and given an output sequence  $O = \{o_1, o_2, \dots, o_\tau\}$ , it is possible to calculate the forward probability  $P_f$  of  $O$ . In doing so, we can determine how likely it is that a particular trained HMM  $\lambda$  has emitted the observed sequence  $O$ . This is defined as the first canonical problem over an HMM.

In our previous research we used an HMM approach to perform a task classification based on observations of haptic data (motion and force signals). Since a discrete HMM was chosen for our implementations, time series data could not be processed directly, but rather had to be represented by a finite alphabet. In [7] we developed a method for an event-triggered feature extraction for time series of haptic data. Output symbols of this feature extraction were passed as discrete observations to a set of trained HMMs, whereby each HMM  $\lambda_i$  represented one of the tasks to be distinguished (in the current example  $T \in \{T2, T3, T4\}$ ). Passing a moving window of observation sequences to these HMMs and solving the first canonical problem for each of them allows calculating their probability  $P_{f_i}$ , which specifies how likely it is that one of them has emitted the observation sequence. In our original implementation the HMM with the highest probability and the corresponding task were selected as result of the task classifier. Interested readers please refer to [7] for a more detailed description of the implemented task classifier and training procedure.

## 2.4 Agreement evaluation

While in our original implementation the HMM with the highest probability  $P_{\max} = \max(P_i)$  for each HMM  $i = 2, 3, 4$  determined the classification result, in this subsection we introduce a method for correcting erroneous task classifications by real-time evaluation of an agreement criterion.

After having determined the probabilities  $P_i$  for each HMM  $\lambda_i, i = 2, 3, 4$ , the classification results are sorted in descent order of the corresponding probabilities and summarized in the vector  $T$ . During normal operation of the classifier, the HMM that most likely emitted  $O$  is used and the corresponding task classification result  $T(1)$  is sent to the assistance unit. However, whenever the agreement criterion detects a disagreement between human operator and assistant, it is interpreted as indicator for a wrong task classification and the task selection block automatically nominates the HMM with the next highest probability and updates the task classification result which is sent to the assistance unit. Our assumption here is that even in case of wrong task classification, the correct task has still high probability. A flowchart showing the proposed classification correction algorithm is given in Fig. 4. We will explain it using an example: Suppose, the operator performs positioning of the object, i.e.  $T(1) = T3$ . The classifier is in *normal mode* and as  $DC = 0$  sends the output  $T(1)$  to the assistance unit. Assuming now, that a new symbol  $O_{i+1}$  recognizes constrained carrying task, such that  $T(1)$  switches to  $T4$ . This wrong classification result is sent to the assistance unit, which activates the assistance function for  $T4$ . This leads to an increase of the interactive accelerations, leading to a rising edge of the  $DC$  signal. The classifier switches to the *correction mode* and outputs the task with the next highest probability  $T(2)$ . We assume, that the correct task has the second highest probability, i.e.  $T(2) = T3$ . During the subsequent loops we observe if  $T(1)$  changes. If so, we switch back again to normal mode. Such a situation is shown in Fig. 5. During the correction mode, we expect that there is some time delay after which the human reacts to the new assistance. Thus,  $DC$  will drop to zero after this adaptation time. We chose 100 ms for the adaptation time. After that, if the signal  $DC$  is still active, this is an indication for a wrong triggered disagreement between human and assistance and consequently the algorithm switches again back to normal mode.

## 2.5 Agreement criterion

In the following paragraph the used agreement criterion is introduced: As shown in [10], interactive forces  $f_i$  can be used to detect, whether human operator and assistant agree in their execution of a task, as they occur if two partners, i.e. human and assistant, push or pull in different directions. They are defined as follows, cf. also

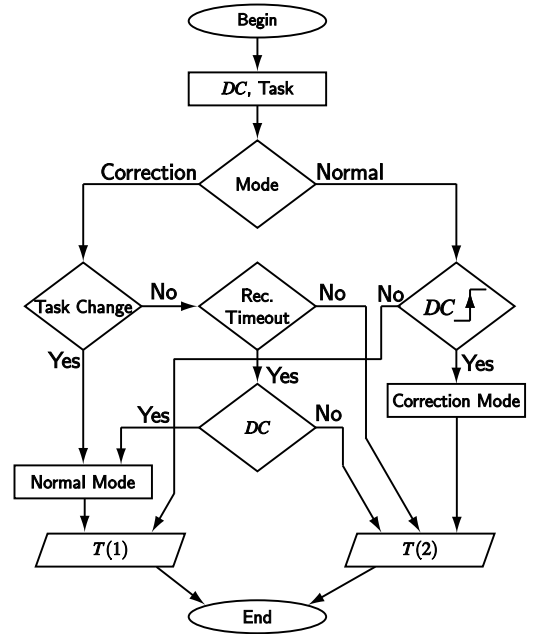


Figure 4: Task correction algorithm:  $T(1)$  is the task for which HMM has the highest probability  $P_{\max}$  and  $T(2)$  is the task with the next lower probability.

Fig. 6:

$$f_i = \begin{cases} f_h & \text{if } \text{sign}(f_h) \neq \text{sign}(f_a) \wedge |f_h| \leq |f_a| \\ -f_a & \text{if } \text{sign}(f_h) \neq \text{sign}(f_a) \wedge |f_h| > |f_a| \\ 0 & \text{else.} \end{cases} \quad (1)$$

In this work, only forces are considered. Yet, the concept is applicable to torques as well. Interactive forces are compressive or tension forces between haptic assistant and human operator that do not result into motion of the object. Whenever the correct task is classified, the assistant either applies forces in the same direction as the operator or slightly counteracts the human applied forces. This results in small interactive forces supporting the actions of the human in a desired way. Whenever a wrong task is classified, an unsuitable assistance function is activated. In this case, the human has to strongly counteract the undesired assistance forces, resulting in large interactive forces. If e.g. transportation is recognized during a carrying task, the human applied forces in the up/down direction are reduced by 90%. In order to compensate the weight of the hard drive, the human will have to apply large forces in the up/down direction. This again leads to large interactive forces, which can be interpreted as disagreement between operator and assistant.

Thus, whenever measured interactive forces cross a pre-determined disagreement threshold  $DT$  in at least one of the translational directions, the disagreement criterion  $DC$  is updated as follows:

$$DC = \begin{cases} 0 & \text{if } |f_{ik}| < DT_k \quad \forall k \in \{x, y, z\} \\ 1 & \text{else.} \end{cases} \quad (2)$$

Agreement between human and assistant is denoted by  $DC = 0$ , while  $DC = 1$  means human and robot disagree.

So far, the agreement criterion can only be used, if an activated assistance function leads to measurable interactive forces. If, however, the assistance function only modifies the position or velocity of the teleoperator without applying the same transformation at operator site (like in  $T4$ ), no interactive forces can be measured. In such cases, we propose an agreement criterion based on the deriva-

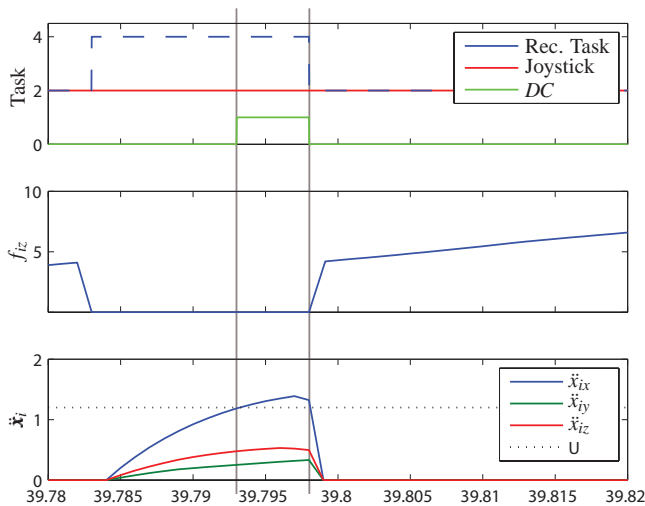


Figure 5: Example of task correction

tive of interactive velocities  $\dot{x}_i$ , which are defined in the same way as the already introduced interactive forces.

It is important to note that the disagreement thresholds can be easily determined from the available data used to train the HMMs by comparing the interactive forces for one assistance function in two situations. In the first situation, the assistance is correctly applied, i.e. the assistance for transportation is applied during a transportation task. In the second situation, the assistance is erroneously applied, i.e. the assistance for transportation is applied during positioning or carrying.

For transportation and positioning, only the z-component of the interactive force vector is evaluated, while for carrying the norm of the interactive acceleration vector is considered. In order to reduce noise, the interactive acceleration signal  $\ddot{x}_i$  was low-pass filtered with a cutoff frequency of 8 Hz.

As for the training procedure of the classifier each task is performed with each assistance function, all required data are given, such that the additional effort to implement the proposed correction method is only slightly increased compared to the original implementation.

**T2 Transportation:** The threshold was selected comparing the interactive forces in a training dataset where the assistance with and without correctly activated type of assistance was used. In a first step the interactive forces in up/down (z) direction are determined if the assistance is applied correctly. In a second step, these interactive forces are compared with interactive forces lying considerably above these values for the case where the assistance is applied erroneously. The threshold was then determined heuristically as to clearly separate interactive forces for both situations leading to  $DT_z^{T2} = 17.8$  N.

**T3 Positioning:** The agreement threshold for positioning is determined in the same way as for transportation. It was found as  $DT_z^{T3} = 19.8$  N.

**T4 Carrying:** Correctly distinguishing carrying from positioning or transportation is crucial, because the implemented velocity amplification adopted while carrying could easily lead to oscillations and instability when applied during constrained manipulation. Such mis-classifications are highly critical for safety of the overall system. They can be detected by evaluating interactive accelerations  $\ddot{x}_i$ . The same procedure as for the other two tasks was used and the threshold was found for all three directions as  $DT = [1.2, 1.2, 1.2]$  Nm/s<sup>2</sup>.

When tuning the thresholds not only the recorded data have to

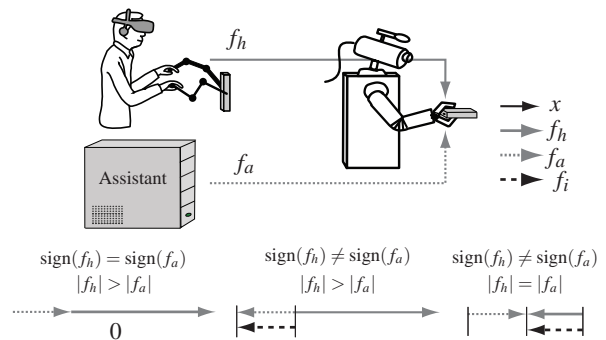


Figure 6: Illustration of interactive forces in one direction between human operator and haptic assistant

be considered, but also the recognition abilities of the classifier in *normal mode*. If a task is classified with a high overall recognition rate we set the corresponding threshold to a high value. Hence, the correction algorithm switches rarely and we prevent wrong disagreement triggering. On the other hand, in setting the thresholds lower, we more often go to the correction mode, which is suitable for a task where the classifier has a low recognition ability.

### 3 EXPERIMENTAL EVALUATION

Finally, the proposed approach was evaluated in a teleoperation scenario. Setup and results are described and discussed in the following subsections.

#### 3.1 Setup

**Apparatus:** The experimental setup used for evaluating the proposed approach is shown in Fig. 7. The hyper-redundant 10 DOF ViShARD10 robotic arm was used as haptic interface. The arm has a large, singularity-free workspace and a high force output capability, see [15] for a detailed performance analysis. On teleoperator site an anthropomorphic 7 DOF robotic arm [16] was used. Both devices are equipped with JR3 6 DOF force/torque sensors mounted at their end-effectors. End-effector positions were obtained by applying the forward kinematics to the measured joint angles. Gravity forces of the end-effectors were compensated in the force measurements. The operator was connected to the haptic interface by means of an aluminum bar which was fixed at the back of his hand. In order to perform manipulation tasks the teleoperator was additionally equipped with a two finger robotic gripper. To open and close this gripper the distance between thumb and index finger of the operator's hand was measured using the commercially available CyberGlove system by Immersion Corp. All controllers ran at a sampling frequency of 1 kHz. Experimental data were recorded at the same frequency. The operator had direct view on the remote site.

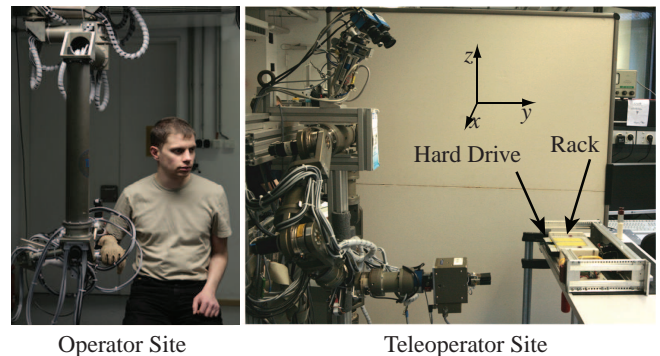


Figure 7: Experimental setup

**Control:** A position-based admittance controller with bilateral force-force exchange as proposed in [17] was implemented. Movements of the single devices were restricted to the 3 translational DOF. On master site, forces originating from the haptic assistance functions  $\mathbf{f}_a$ , the remote environment  $\mathbf{f}_e$ , and forces applied by the human operator  $\mathbf{f}_h$  were summed up and used as input for the virtual admittance of the local position-based admittance controller. For the carrying task, additionally velocities commanded by the assistance functions  $\dot{\mathbf{x}}_a$  were added to the desired velocities  $\dot{\mathbf{x}}_s^d$  of the local position controller of the slave. The two desired dynamics for master and slave were as follows

$$\begin{aligned}\mathbf{f}_h + \mathbf{f}_a - \mathbf{f}_e &= (\mathbf{M}_n + \mathbf{M}_a)\ddot{\mathbf{x}}_m^d + (\mathbf{D}_n + \mathbf{D}_a)\dot{\mathbf{x}}_m^d \\ \mathbf{f}_h + \mathbf{f}_a - \mathbf{f}_e &= (\mathbf{M}_n + \mathbf{M}_a)\ddot{\mathbf{x}}_s^d + (\mathbf{D}_n + \mathbf{D}_a)(\dot{\mathbf{x}}_s^d + \dot{\mathbf{x}}_{sa}^d)\end{aligned}$$

where  $\mathbf{M}_{n/a}, \mathbf{D}_{n/a}$  are diagonal matrices, representing virtual mass and damping characteristics of nominal controller and assistant, respectively, and  $\ddot{\mathbf{x}}_{m,s}^d$  are the desired accelerations of the master and slave device. The desired positions for master and slave device were tracked using high-gain PD-controllers operating in joint space. The nominal values of  $\mathbf{M}_n, \mathbf{D}_n$  were chosen as 12 kg and 70 Ns/m for each direction. These values were selected from a set of parameters for stable interaction, which were found using the parameter space approach as described in [17].

### 3.2 Results

The overall task was performed 25 times by one expert operator without correcting the task classification, referred to as classical approach, and 25 times using the correction approach. In order to reduce learning effects, the approach was changed after 5 trials. In addition, for comparing actually performed task and classified task, the operator indicated the currently performed task using a joystick. The signals from the joystick, denoted as  $T_j$ , serve as a baseline for the actual classified task, denoted as  $T_c$ , can be compared to. However, as the transition from one task to another cannot be determined exactly, data within a correction window of 0.5 s before and after a new task entered via the joystick were neglected. Table 1 summarizes the classification results for both approaches. Results are given for each task separately as well as for the task as a whole. Furthermore, the correct classification rate for selecting carrying while performing a positioning or transportation task is reported. This rate is especially important for safety, as applying the assistance function designed for T4 can lead to instability when applied in constrained manipulation tasks such as positioning or transportation.

The values  $\mu$  and  $\sigma$  are the mean and standard deviation of the classification rates  $CR$ , obtained for each trial. The classification rate is calculated as the number of correct classifications results  $CC$  divided by the total number of classification results, i.e. the number of samples in a trial  $L$  times 100:

$$CR = 100 \frac{CC}{L}.$$

Thus, a  $CR$  value of 100 % means, that the task was correctly classified at all times.

As can be seen from the results, the new approach outperforms the classical approach for all tasks except carrying. Furthermore, a very important improvement can be seen for safety critical tasks, where the classification rates increase from 84.04% to 94.42% using the proposed approach, cf. last line of Table 1. Also the standard deviation for the safety critical tasks are smaller for the new approach than for the classical approach indicating a more stable classification.

Thus, the main hypothesis of an improved classification rate of the new approach over the classical approach can be generally confirmed. For carrying, the threshold for the agreement criterion is

Tasks	Classical Approach		New Approach	
	$\mu_c$ [%]	$\sigma_c$ [%]	$\mu_n$ [%]	$\sigma_n$ [%]
Transportation	61.36	16.01	83.42	14.59
Positioning	84.80	13.43	92.72	9.40
Carrying	94.90	6.98	92.05	12.79
All	77.21	7.83	87.74	9.32
T4 during T2 or T3	84.04	12.59	94.42	7.71

Table 1: Mean and standard deviation of correct classification rates for old and new approach

set in a conservative way, such that the detection of wrongly classified carrying tasks during positioning and transportation are detected stably, i.e. with a high probability. This leads to an increase in stability, as the classification of carrying during positioning or transportation leads to oscillations easily. If the task classification does not switch back to positioning or transportation fast enough, the wrong classification can even lead to instability. On the contrary, however, the conservative agreement threshold can lead to a decrease in classification for carrying, as disagreement during the carrying task may be wrongly triggered. As carrying can be safely performed with all assistance functions, this mis-classification is not critical. In summary, an overall improvement in the classification results is obtained and stability is increased.

### 4 CONCLUSION

In this paper, an approach for improving task classification for a human-machine collaborative teleoperation system was presented. Starting from a classical HMM-based classifier implemented in our previous research, a method for correcting erroneous task classifications by evaluating a disagreement criterion was introduced. A criterion evaluating interactive forces was proposed and used to distinguish between situations in which human and assistant agree or disagree in their execution of the task. Using disagreement as indicator for the activation of an unsuitable or suboptimal assistance, erroneous task classifications were identified and the classification result was corrected. The proposed approach leads to significant improvements in task classification along with a low implementation effort. Preliminary experimental results showed an average overall improvement in task classifications of 10% compared to the classical approach without correction as well as for safety critical tasks. Further, for safety critical tasks, a smaller standard deviation was observed for the proposed approach compared to the classical approach indicating a more stable classification.

Future work consists in the extension of this approach to a broader class of tasks and assistance functions as well as in a user study to statistically confirm found results with multiple users.

### REFERENCES

- [1] C. Passenberg, A. Peer, and M. Buss, "A survey of environment-operator- and task-adapted controllers for teleoperation systems," *Mechatronics: Special Issue on Design and Control Methodologies in Telerobotics*, vol. 20, pp. 787–801, 2010.
- [2] B. Hannaford and P. Lee, "Hidden Markov Model Analysis of Force/Torque Information in Telem Manipulation," *The International Journal of Robotics Research*, vol. 10, pp. 528–539, 1991.
- [3] M. Li and A. Okamura, "Recognition of operator motions for real-time assistance using virtual fixtures," in *11th Symposium on Haptic Interfaces for Virtual Environment and Teleoperator Systems*, pp. 125–131, 2003.
- [4] W. Yu, R. Alqasemi, R. Dubey, and N. Pernalet, "Telem Manipulation assistance based on motion intention recognition," in *IEEE International Conference on Robotics and Automation*, pp. 1121–1126, 2005.

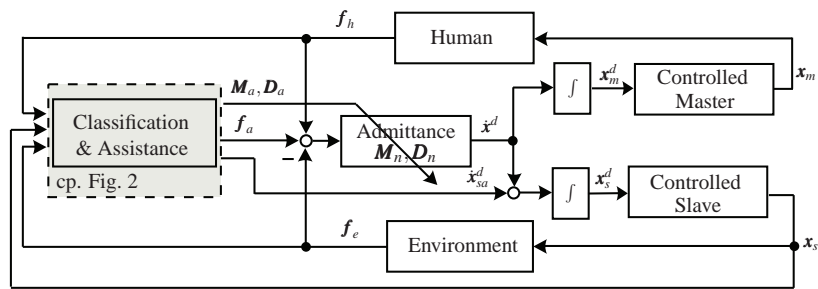


Figure 8: Overall control structure

- [5] D. Kragic, P. Marayong, M. Li, A. M. Okamura, and G. D. Hager, "Human-Machine Collaborative Systems for Microsurgical Applications," *The International Journal of Robotics Research*, vol. 24, pp. 731–741, 2005.
- [6] D. Aarno, S. Ekvall, and D. Kragic, "Adaptive virtual fixtures for machine-assisted teleoperation tasks," in *IEEE International Conference on Robotics and Automation*, pp. 1139–1144, 2005.
- [7] N. Stefanov, A. Peer, and M. Buss, "Online intention recognition for computer-assisted teleoperation," in *IEEE International Conference on Robotics and Automation*, pp. 5334–5339, 2010.
- [8] L. Parra, C. Spence, A. Gerson, and P. Sajda, "Response error correction - a demonstration of improved human-machine performance using real-time EEG monitoring," *IEEE Transactions on Neural Systems and Rehabilitation Engineering*, vol. 11, pp. 173–177, 2003.
- [9] P. Ferrez and J. del R. Millan, "Error-related EEG potentials generated during simulated brain-computer interaction," *IEEE Transactions on Biomedical Engineering*, vol. 55, pp. 923–929, 2008.
- [10] C. Passenberg, R. Groten, A. Peer, and M. Buss, "Towards real-time haptic assistance adaptation optimizing task performance and human effort," in *Worldhaptics*, 2011, accepted.
- [11] O. Khatib, "Real-Time Obstacle Avoidance for Manipulators and Mobile Robots," *The International Journal of Robotics Research*, vol. 5, pp. 90–98, 1986.
- [12] P. Aigner and B. McCarragher, "Human integration into robot control utilising potential fields," in *IEEE International Conference on Robotics and Automation*, pp. 291–296, 1997.
- [13] L. Rabiner and B. Juang, "An introduction to hidden markov models," *ASSP Magazine, IEEE*, vol. 3, pp. 4–16, Jan 1986.
- [14] T. Takeda, K. Kosuge, and Y. Hirata, "HMM-based dance step estimation for dance partner robot - MS DanceR," in *International Conference on Intelligent Robots and Systems*, pp. 3245–3250, Aug. 2005.
- [15] M. Ueberle, N. Mock, and M. Buss, "Vishard10, a novel hyper-redundant haptic interface," in *12th International Symposium on Haptic Interfaces for Virtual Environment and Teleoperator Systems*, pp. 58–65, 2004.
- [16] B. Stanczyk and M. Buss, "Development of a telerobotic system for exploration of hazardous environments," in *IEEE/RSJ International Conference on Intelligent Robots and System*, 2004.
- [17] A. Peer and M. Buss, "Robust stability analysis of a bilateral teleoperation system using the parameter space approach," in *IEEE/RSJ International Conference on Intelligent Robots and Systems*, pp. 2350–2356, Sept. 2008.